Table of Contents

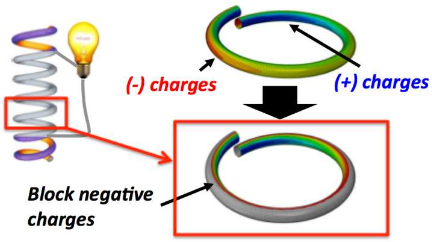

We designed and fabricated a high performance spring-type piezoelectric energy harvester that selectively collects current from the inner part of spring shell.

RSC Advances RSCPublishing

COMMUNICATION

Selective current collecting design for spring-type energy harvesters

Cite this: DOI: 10.1039/x0xx00000x

Dongjin Kim,[a,b] Hee Seok Roh,[c] Yeontae Kim,[a] Kwangsoo No[a]* and Seungbum Hong[a,b]*

Received 00th January 2012,
Accepted 00th January 2012

DOI: 10.1039/x0xx00000x

www.rsc.org/ees

Here we present a high performance spring-type piezoelectric energy harvester that selectively collects current from the inner part of spring shell. We analyzed the main reason behind the low efficiency of the initial design using finite element models and proposed a selective current collecting design that can considerably improve the electrical conversion efficiency of the energy harvester. We found that the newly designed energy harvester increases the output voltage by 8 times leading to an output power of 2.21 μW under impulsive load of 2.18 N when compared with the conventional design. We envision that selective current collecting design will be used in spring-based self-powered active sensors and energy scavenging devices.

The mechanical energy generated by a vibrating structure and a moving object is one of the most ubiquitous energies that can replace or add to the existing power sources such as batteries that have a limited energy storage capacity and lifespan.[1-5] Energy scavenging from the mechanical energy is generally made through one of three conversion mechanisms such as electrostatic, electromagnetic, and piezoelectric effect.[6] Although each conversion mechanism has advantages in different applications, piezoelectric conversion has received the most attention for use as sustainable electrical power supplies for portable and wireless electronics as well as wearable devices.[7] The advantage of piezoelectric conversion is that they are able to directly convert mechanical energy into electrical power. In other words, the piezoelectric conversion needs no complex geometries or numerous additional components, which lead to a simpler device design in comparison to other mechanisms.[8] Therefore, piezoelectric energy harvesting (PEH) has been considered and explored as a simple technology able to scavenge electrical energy converted from mechanical energy in our surroundings.[9-12]

Piezoelectric energy harvesting systems (PEHSs) can be classified into two types based on whether a piezoelectric harvester (PEH) is newly installed as a standalone device or embedded in the system. The first one is installed as a new stand-alone PEH; this type of PEH are usually installed at a spot where the mechanical vibration is generated, adding a working volume of PEH to the system. Most of the stand-alone PEHs consist of 2-D structures such as beam, plate and film.[5,13-15] Although PEHSs of this type are simpler and less spacious than the systems using other mechanisms such as electromagnetic and electrostatic conversion, additional space and components for the PEHs are still required for scavenging energy. Moreover, the size of the PEH could only be reduced to a certain size due to the fact that the harvested energy changes in accordance with the size of the PEH. The second type uses the existing structure as the substrate for the PEH. Such embedded systems do not need significant additional space and weight for the PEH, which enable us to convert otherwise wasted volume and energy into useful ones.

Recently, embedded PEHSs using spring-type PEHs have received attention for their applicability to existing structures without the needs to either significantly modify the design or add volume.[16,17] Mechanical springs have been widely used as the component of machineries, vehicles or constructions for damping the external shock and stress. A few research groups developed three-dimensional spring-type PEHs using P(VDF-TrFE) film[16] or ZnO nanowires film,[17] which could effectively generate electricity using applied mechanical stress. However, there is a remaining issue in the earlier works of spring-type PEHs (SPEHs), which is their low electrical conversion efficiency.

Herein, we report the main reason behind the low efficiency using finite element models and propose the selective current collecting design that can considerably improve the electrical conversion efficiency of the SPEHs when compared to the conventional ones reported in the literature.

We conducted Finite Element Analysis (FEA)[18] using ABAQUS 6.13 to calculate the stress distributions on P(VDF-TrFE) film on a spring. Shell elements were used for the P(VDF-TrFE) film because the film thickness was small enough compared to the other dimensions. Therefore, we only obtained in-plane stresses such as σ_{11}, σ_{22}, and σ_{12} but ignored stresses in thickness direction. In addition, it is well known that piezoelectric materials generate electric voltages in response to applied mechanical loads. In case of thin P(VDF-TrFE) film, only σ_{11} and σ_{22} are related to the generation of voltages, where 11- and 22- directions indicate axial and circumferential directions of spring wire, respectively.[16]

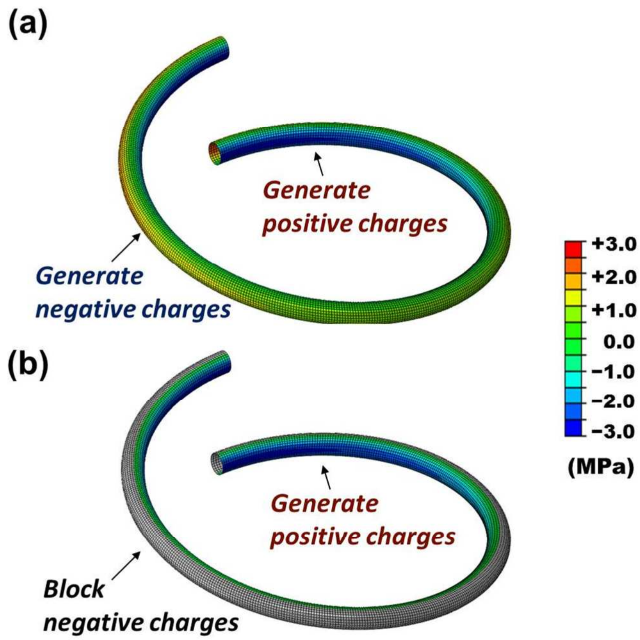

Figure 1 Stress distributions on (a) P(VDF-TrFE) thin film coated on the spring (original design) and (b) P(VDF-TrFE) thin film coated only inner part of the spring (new design). When the ferroelectric polymer is poled toward inner (the spring) direction, compression force generates positive charges and tensile force generates negative charges.

Figure 1a shows the stress distribution in P(VDF-TrFE) film deposited on the spring. We calculated σ_{11} and σ_{22} in P(VDF-TrFE) film and visualized their sum in Figure 1a that is responsible to electric current. From the simulation result we found that there are two main current components with opposite polarities through the outer and the inner parts of the SPEH. The shell element in the outer part of the spring is subject to a positive force (tension) while the shell element in the inner part of the spring is subject to negative force (compression). Therefore, each of the opposite forces generates electrical charges with opposite polarities.

When the spring is loaded with compressive force of 3.08 N, the forces applied to the elements in the outer and the inner parts of the spring are 61.5 N and -68.6 N, respectively, as listed in Table 1. As a result, the net force is -7.1 N, which the SPEH is subject to and contributes to the overall generated electrical current from the SPEH.

Based on the analysis above, we propose a new design for SPEH to enhance the conversion of mechanical force to electrical charges. The main feature of the new design is to block the current from the outer part of spring and selectively collects the current from the inner part of the spring. In order to realize the design, we coated the outer part of P(VDF-TrFE) film with an electrically insulating film. While the insulating film blocks the current from the outer part of the spring, the SPEH generates an electrical current induced by the

Table 1 Summations of forces applied on the elements by element.

Design	Summation on element by element (N/coil)		
	Positive	Negative	Net
Original	61.5	-68.6	-7.1
New	0.0	-68.6	-68.6

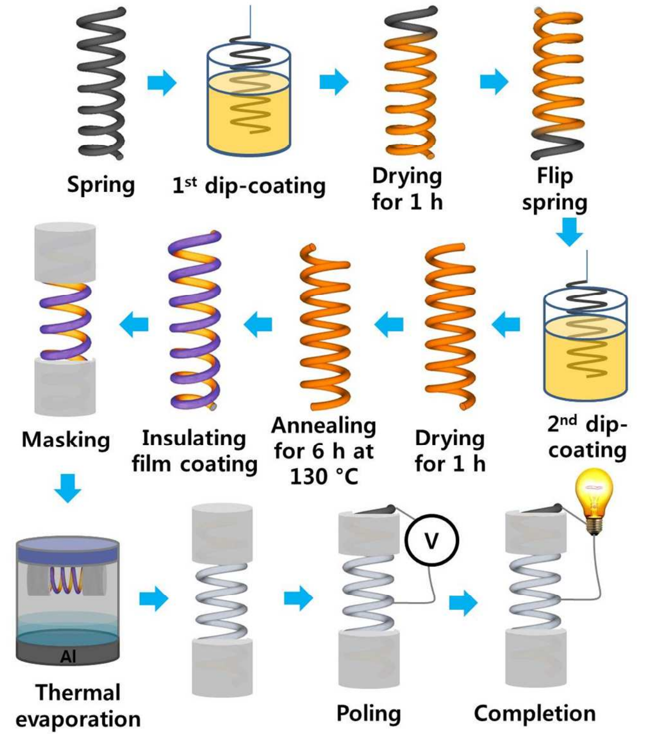

Figure 2 Schematics of the fabrication process of newly designed SPEH.

negative force acting on the inner part of the spring as shown in Figure 1b. As a result, when the newly designed SPEH is loaded with compressive force of 3.08 N, the net force acting on the inner part is -68.6 N which increases the output power by 9.67 times when compared with the initially designed SPEH.

Figure 2 shows the schematic of fabrication process to make SPEH with the selective current collecting design. Firstly, P(VDF-TrFE) solution and a spring were prepared. The precursor solution was prepared by dissolving 20 wt% P(VDF-TrFE) (VDF:CH2-CF2/TrFE:CHF-CF2, 75/25) in methyl ethyl ketone solvent (MEK). Stainless steel spring was a commercially available one (Hyundai Spring, Inc.), with a wire diameter of 0.89 mm, an outer spring diameter of 15.03 mm and a length of 40.28 mm, respectively. The spring had 6 turns. The spring constant was measured by placing a mass of 500 g at the end of the spring. Before the dip-coating process, the spring was cleaned using acetone and ethanol and then dried for 1 hour in vacuum of less than 1 kPa. The spring was immersed into the solution for 30 s. The spring was then withdrawn from the solution at a pulling speed of 10 mm/min using the dip-coater (TL0.01, MTI Corporation, Inc.). The coated P(VDF-TrFE) was left to dry for 1 h in ambient condition. To have a uniform coating of P(VDF-TrFE) film on the spring, we flipped the spring upside down and repeated the coating process. Then, we annealed the coated spring to increase the crystallinity of P(VDF-TrFE) film at 130°C for 6 h in ambient condition. After cooling the spring to room temperature, we used the nail polish solution (nail polish, ECO TOP COAT, Innisfree Inc.) to form an insulating film on the outer part of the spring. After drying the spring for 1 h, we masked both ends of the spring using Teflon tape while leaving the middle one third of the spring unmasked. Afterwards, we coated Al electrode on top of the spring by thermal evaporation. To obtain uniform and conformal coating on the spring, we repeated the Al coating process while rotating the spring about its long axis with an interval of 120˚ for three times. Finally, we removed part of the Teflon mask to electrically connect to the core electrode, which is the spring itself,

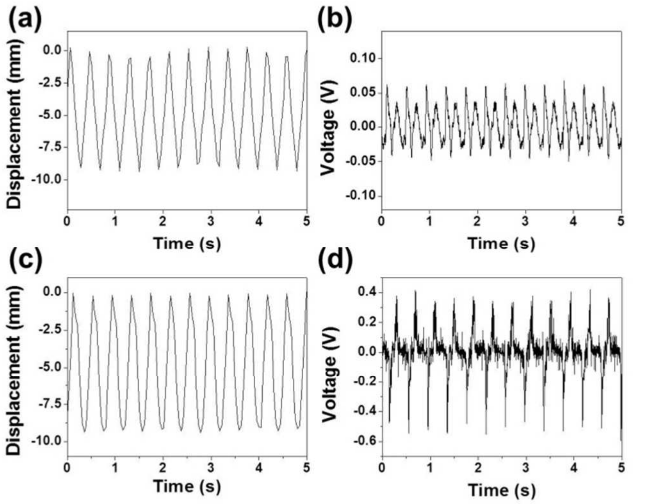

Figure 3 Plots of (a) vertical displacement of the original SPEH under cyclical compression stress, and (b) resulting output voltage signal generated as a function of elapsed time. Comparative plots of (c) vertical displacement of the newly designed SPEH under cyclical compression stress, and (d) resulting output voltage signal generated as a function of elapsed time.

and poled the P(VDF-TrFE) film between core-electrode and surface-electrode with a bias voltage of 400 V for 1 hour using the high voltage DC power supplier (Series FC, Glassman High Voltage, Inc.).

We conducted a comparative experiment between the original and the new designs to evaluate the improvement of the performance in terms of the output voltage generated by the applied force to the spring. In addition to the SPEH with the selective current collecting design ("new design), we fabricated an SPEH using the process described in our previous report[16] and designated it as the original design. We compared the output voltages from both the original and the new designs using the same cyclic displacement condition as shown in Figures 3a and c.

In the original design, the average amplitude of displacement wave was 4.52 mm (standard deviation (SD) = 0.11 mm) under applied vertical force of up to 3.05 N (spring constant was 337.9 N/m) while the frequency of the wave was 2.43 Hz. Figure 3b shows the output voltage signal from the SPEH under the applied cyclical vertical force. We were able to collect the output voltage signals from the SPEH using a digital oscilloscope. The average high and low peak voltages were 0.061 V (SD = 0.029 V) and -0.045 V (SD = 0.026 V), respectively. The average peak-to-peak voltage was 0.106 V (SD = 0.0049 V).

In the new design, the average amplitude of displacement wave was 4.56 mm (SD = 0.06 mm) under applied vertical force of up to 3.08 N while the frequency of the wave was 2.47 Hz. The average high and low peak voltages were 0.371 V (SD = 0.029 V) and -0.514 V (SD = 0.0029 V), respectively as shown in Figure 3d. The average peak-to-peak voltage was 0.885 V (SD = 0.038 V), of which value is 8.22 times higher than that of the original design.

The simulation result using FEA predicts that the selectively collecting current design increases the output power by about 9.67 times based on the ratio of net force acting on the original and the new designs, which is in a good agreement with the experimental results. We think that the discrepancy between the experimental and simulation results resulted from the incomplete shielding effect of the insulating film.(See supplementary information).

We measured the output voltage generated by the SPEH under an impulsive load by dropping a weight of 25 g from various heights as

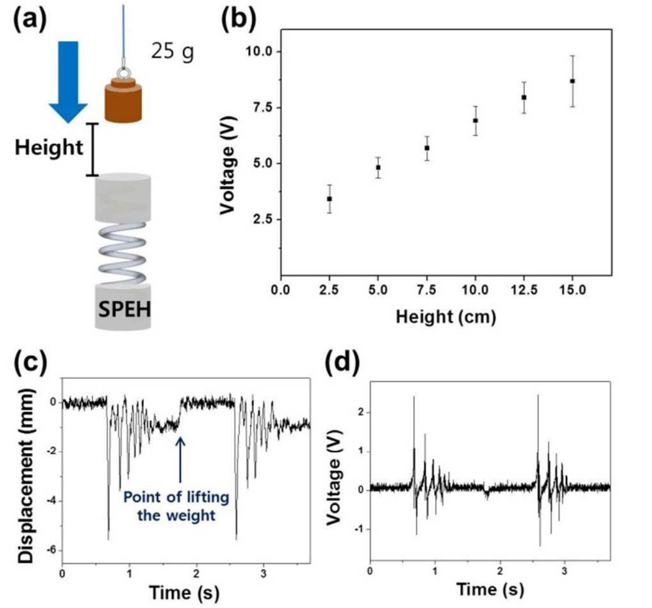

Figure 4 (a) Schematic diagram of the experiment in which the SPEH is impacted by a descending weight of 25 g. (b) Plots of average peak-to-peak voltages generated from SPEH as a function of initial gap height between the weight and the SPEH. Error bars represent the standard deviations. Plots of (c) vertical displacement of the SPEH when impacted from the height of 5 cm, and (d) resulting output voltage signal generated as a function of elapsed time.

shown in Figure 4a. Figure 4b shows the plots of the average peak-to-peak voltage generated from the SPEH as a function of descending height. We found that the output voltage increased linearly with an offset at 0 cm as the height increased.

Figure 4c shows the plots of the vertical displacement of the new design SPEH induced by the impact of the falling weight of 25 g from a height of 5 cm, which leads to a displacement of up to 5.7 mm. Figure 4d shows the output voltage signal generated as a function of the elapsed time. The maximum average peak to peak voltage was 4.82 V (SD = 0.47 V).

We measured the output voltage generated by the SPEH as a function of the load resistance in order to find the optimal electrical loading condition to maximize the output power. The output voltages were measured under an impulsive load by dropping a weight of 25 g from a height of 5 cm. Figure 5a shows the plots of the average peak-to-peak voltage generated by the SPEH. We found that the output voltage increased monotonously as the resistance increased. We calculated the output power using the output voltage and the load resistance, of which plot is shown in Figure 5b. The SPEH generated maximum peak power of 2.21 μW under impulsive load of 2.18 N when the load resistance was 6.6 MΩ.

The output power of 2.21 μW is the highest record reported from SPEHs due to several reasons including our new design of selective current collection and the unique way to collect the electricity via impact experiments. There are currently two prior reports on the spring-type energy harvesters, and one from Wang's group reported open-circuit voltage of up to 0.3 V and short-circuit current of up to 8 nA under the external force of 15.2 N, which results in a peak power of about 2.4 nW, which is about ten times smaller than the peak power of 26.4 nW obtained from our new design under similar type of low frequency cyclic loading.

In conclusion, we designed a high performance spring-type piezoelectric energy harvester that selectively collects current from

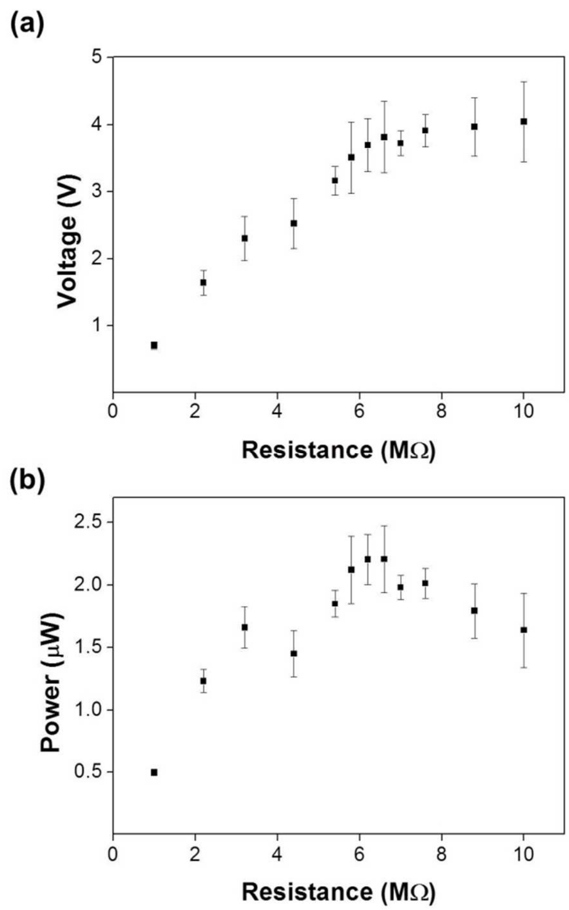

Figure 5 Plots of (a) output peak-to-peak voltage and (b) resulting output power generated from SPEH as a function of the load resistance. Error bars represent the standard deviations. The SPEH generated maximum peak power up to 2.21 μW under impulsive load of 2.18 N at the load resistance of 6.6 MΩ.

inner part of spring shell. Our design was based on the finding that there are currents with opposite polarities between outer and inner parts of spring shell within SPEH that results in decrease of output power. We found that the newly designed SPEH generates peak power up to 2.21 μW under impulsive load of 2.18 N due to the selective current collecting design that increases the output voltage by 8.22 times. We envision that selective current collecting design will be used in spring-based self-powered active sensors and energy scavenging devices.

Acknowledgements

This research was supported by the Converging Research Center Program (No. 2011-K000674) and Mid-career Researcher Program (No. 2010-0015063) through the National Research Foundation (NRF) funded by the Ministry of Education, Science and Technology (MEST), Korea. Work at Argonne National Laboratory (D.K., S.H., and H.R., design of selective current collection scheme, simulation of stress and charge, data analysis and writing of manuscript) was supported by UChicago Argonne, a U.S. DOE Office of Science Laboratory, operated under Contract No. DE-AC02-06CH11357.

Notes and references

[a] Department of Materials Science and Engineering, KAIST, Daejeon 305-701, Korea, Email: seungbum@kaist.ac.kr, ksno@kaist.ac.kr
[b] Materials Science Division, Argonne National Laboratory, Lemont, IL 60439, USA, Email: hong@anl.gov
[c] Nuclear Engineering Division, Argonne National Laboratory, Lemont, IL 60439, USA

Electronic Supplementary Information (ESI) available: [details of any supplementary information available should be included here]. See DOI: 10.1039/c000000x/

1 S. P. Beeby, M. J. Tudor and N. M. White, *Meas. Sci. Technol.*, 2006, **17**, R175.
2 L. C. Rome, L. Flynn, E. M. Goldman and T. D. Yoo, *Science*, 2005, **309**, 1725.
3 J. M. Donelan, Q. Li, V. Naing, J. A. Hoffer, D. J. Weber and A. D. Kuo, *Science*, 2008, **319**, 807.
4 A. Erturk and D. J. Inman, Piezoelectric energy harvesting, Wiley, 2011, Chapter 1.
5 L. B. Kong, T. Li, H. H. Hng, F. Boey, T. Zhang, S. Li, *Waste Energy Harvesting*, Springer, Berlin, 2014, Chapter 2.
6 K. A. Cook-Chennault, N. Thambi and A. M. Sastry, *Smart Mater. Struct.*, 2008, **17**, 043001.
7 N. Soin, T. Shah, S. Anand, J. Geng, W. Pornwannachai, P. Mandal, D. Reid, S. Sharma, R. Hadimani, D. Bayramol and E. Siore, *Energy Environ. Sci.*, 2014, **7**, 1670.
8 J. A. Paradiso and T. Starner, *IEEE Pervasive Comput.*, 2005, **4**, 18-27.
9 S. Priya, *J. Electroceram.*, 2007, **19**, 165.
10 S. P. Beeby, R. N. Torah, M. J. Tudor, P. Glynne-Jones, T. O'Donnell, C. R. Saha and S. Roy, *J. Micromech. Microeng.*, 2007, **17**, 1257
11 C. Sun, J. Shi, D. J. Bayerl and X. Wnag, *Energy Environ. Sci.*, 2011, **4**, 4508.
12 Y. Qi and M. C. McAlpine, *Energy Environ. Sci.*, 2010, **3**, 1275.
13 H. A. Sodano and D. J. Inman, *J. Intell. Mater. Syst. Struct.*, 2005, **16**, 799.
14 A. Hajati and S. G. Kim, *Appl. Phys. Lett.*, 2011, **99**, 083105.
15 A. Erturk and D. J. Inman, *Smart Mater. Struct.*, 2009, **18**, 025009.
16 D. Kim, S. Hong, D. Li, H. S. Roh, G. Ahn, J. Kim, M. Park, J. Hong, T. Sung and K. No, *RSC Adv.*, 2013, **3**, 3194.
17 L. Lin, Q. Jing, Y. Zhang, Y. Hu, S. Wang, Y. Bando, R. Han and Z. L. Wang, *Energy Environ. Sci.*, 2013, **6**, 1164.
18 Z. S. Ma, Y. C. Zhou, S. G. Long, C. Lu, *Inter. J. Plast.* 2012, **34**, 1.

